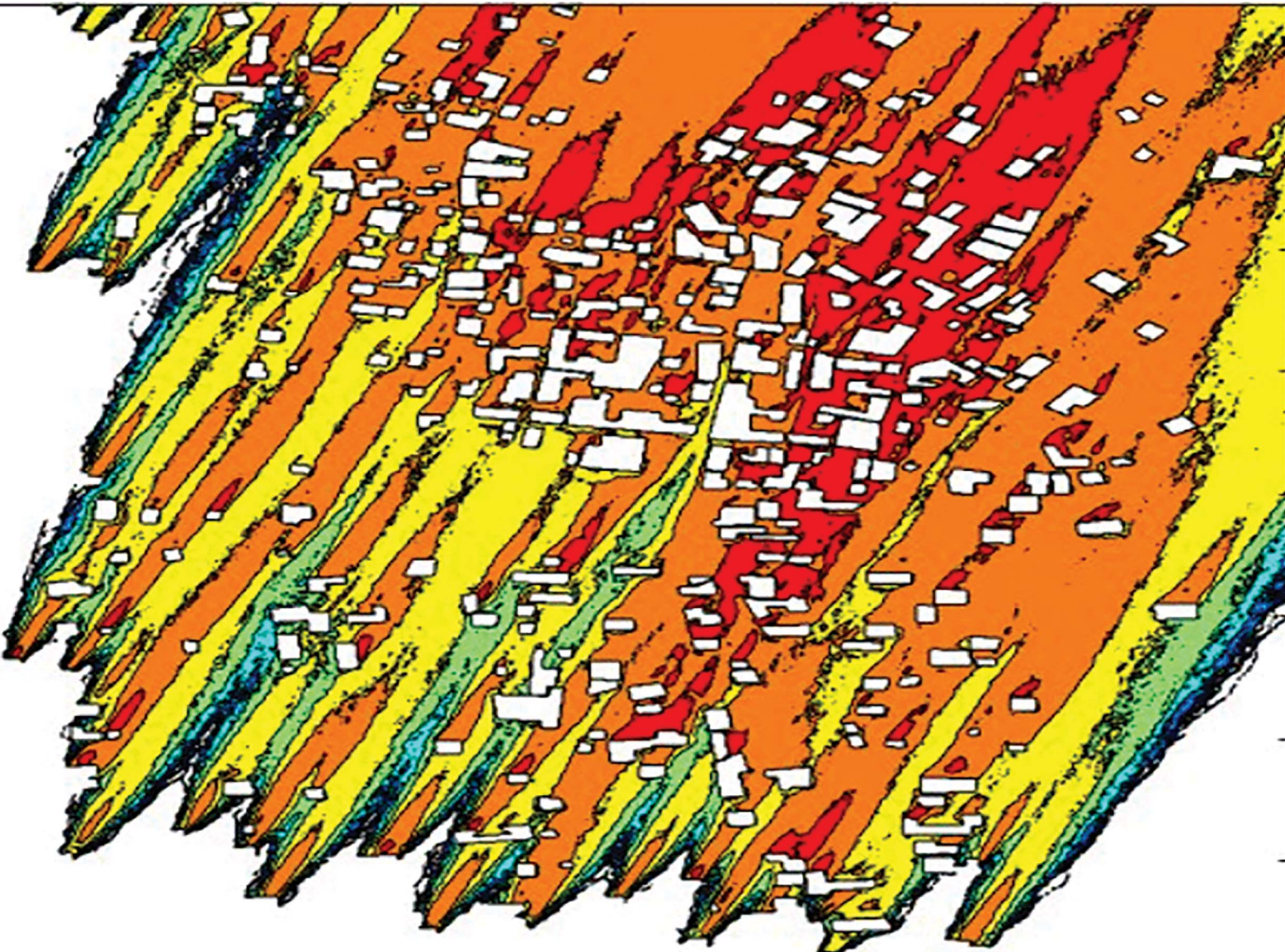


# Environmental Science Atmospheres

[rsc.li/esatmospheres](https://rsc.li/esatmospheres)



ISSN 2634-3606



Cite this: *Environ. Sci.: Atmos.*, 2025, 5, 171

## Estimation of neighborhood scale PM<sub>2.5</sub> impacts in rural towns in the Purepecha region of Mexico†

Yucheng He, <sup>a</sup> Sanika R. Nishandar, <sup>a</sup> Rufus D. Edwards, <sup>\*b</sup> Belén Olaya-García, <sup>c</sup> Montserrat Serrano-Medrano, <sup>c</sup> Víctor M. Ruiz-García, <sup>ce</sup> Víctor Berrueta, <sup>d</sup> Marko Princevac <sup>a</sup> and Omar Masera <sup>c</sup>

The impact of cooking with solid fuels on neighborhood-scale PM<sub>2.5</sub> concentrations in rural towns and communities is poorly quantified due to the lack of credible ground-level monitoring sites and spatial heterogeneity at a scale that is below the resolution of remote sensing GEOS-Chem hybrid models. Emissions of PM<sub>2.5</sub> from use of open fires for cooking in rural Mexico are known to cause poor indoor air quality. The effectiveness of different intervention strategies to reduce such pollution exposures also varies because of different local building densities and source intensities. In this study, the effectiveness of stove intervention strategies on the neighborhood-scale PM<sub>2.5</sub> concentrations were evaluated in a village Cucuchucho, located in the Purepecha highlands of Mexico. The Quick Urban & Industrial Complex (QUIC) is deployed in the assessment. The model's performance in simulating interactions between pollutants and flow around building structures is validated through comparison with a water channel experiment, which shows good quantitative agreement. The case study simulation results demonstrate that upstream households contributed ~30% of concentrations, and current trends will not meet WHO air quality guidelines or interim targets. The magnitude of neighborhood-scale PM<sub>2.5</sub> concentrations depends on the intervention and community structure. Based on these simulations, a statistical model is presented to estimate ambient neighborhood PM<sub>2.5</sub> pollution concentrations for more communities at a regional level. The statistical model allows neighborhood PM<sub>2.5</sub> pollution to be included in estimates of health burdens from household pollution in Mexico using readily accessible community parameters.

Received 12th June 2024  
Accepted 4th December 2024

DOI: 10.1039/d4ea00082j  
[rsc.li/esatmospheres](http://rsc.li/esatmospheres)

### Environmental significance

In rural Mexico, there is considerable household energy demand from solid fuel biomass burning, leading to the emission of PM<sub>2.5</sub> known to cause poor air quality. The effectiveness of intervention strategies necessitates meticulous quantification before investment and promotion. However, the air quality in these towns and communities is rarely assessed due to the absence of credible ground-level monitoring and the limited resolution of satellite systems. The current study employs computational modeling to quantify PM<sub>2.5</sub> emissions under various interventions in rural areas. This analysis can serve as a reference for policymakers aiming to achieve environmental equity. Another significant contribution of this work is its focus on ambient neighborhood-scale emission quantification. To the author's knowledge, no study has explored this particular topic.

## 1 Introduction

High indoor PM<sub>2.5</sub> exposures in rural populations in Mexico that rely on solid biomass fuels in traditional stoves are well documented, with large-scale interventions of chimney stoves a part of social programs to reduce health impacts.<sup>1–3</sup> Lean and sustainable interventions to mitigate the environmental and health impacts of use of solid fuels for cooking heating and lighting are a key component of Sustainable Development Goal 7. The selection of different intervention choices to mitigate health impacts, however, has frequently been guided by potential benefits that reflect unrealistic choices on the exclusive use of the intervention in daily cooking activities. This approach often lacks consideration of impacts on neighboring

<sup>a</sup>Department of Mechanical Engineering, Marlan and Rosemary Bourns College of Engineering, University of California Riverside, CA 92521, USA

<sup>b</sup>Department of Environmental and Occupational Health, Joe C. Wen School of Population and Public Health, University of California Irvine, Room 1361 SE II, CA 92697, USA. E-mail: [edwardsr@uci.edu](mailto:edwardsr@uci.edu)

<sup>c</sup>Instituto de Investigaciones en Ecosistemas y Sustentabilidad, Universidad Nacional Autónoma de México (UNAM), Morelia, Michoacán 58190, Mexico

<sup>d</sup>Universidad Intercultural Indígena de Michoacán, Pátzcuaro, Michoacán, 61614, Mexico

<sup>e</sup>Consejo Nacional de Humanidades, Ciencias y Tecnologías, Mexico

† Electronic supplementary information (ESI) available. See DOI: <https://doi.org/10.1039/d4ea00082j>



houses that do not opt to use the intervention, resulting in unrealistic expectations and exposure reductions that do not materialize in randomized controlled trials.<sup>4</sup> The contributions of cooking with solid fuels to neighborhood-scale PM<sub>2.5</sub> concentrations in rural towns are poorly quantified. They are not part of global frameworks to assess disease burdens as they are at a spatial scale that is below the resolution of current global PM<sub>2.5</sub> assessment methods. In current global disease assessments, exposures to PM<sub>2.5</sub> air pollution are estimated by combining indoor and outdoor models. Indoor air pollution is estimated by solid fuel use while outdoor ambient pollution is from high-resolution satellite information combined with a GEOS-Chem global 3D model. The model results are usually calibrated by ground level fixed monitoring stations.<sup>5-7</sup> Data inferred from the satellite observations in most locations, however, do not have sufficient resolution to capture the impact of near-field turbulence caused by buildings on the pollution distribution. Vortices developed in the building wakes may trap local emitted pollutants as well as upstream community emitted pollutants in close proximity to the building envelope, which are available for subsequent infiltration based on indoor ventilation rates and structural orifices.<sup>8,9</sup>

Stove stacking refers to the practice of households using multiple types of stoves or cooking devices simultaneously or interchangeably. This often occurs in areas where people are transitioning from traditional biomass stoves to cleaner, more efficient stoves.<sup>10</sup> Realistic assessment of stove stacking, or the degree to which multiple stoves and fuels are used, can significantly impact the choice of intervention strategy to reduce the burden of air pollution in communities.<sup>10</sup> The choice of the optimal clean stacking combination to deliver health benefits may vary between communities, depending on local/upstream pollution impacts, topography, ground roughness, predominant wind direction/speed, immediate building packing density, building morphology, and chimney height.<sup>9,11</sup> Understanding which clean stacking combinations are more suitable to the packing densities of homes in different built communities remains a critical priority, along with developing the approach to incorporate health impacts from neighborhood pollution into regional burden of disease assessment.

Rather than predefining a “clean stacking combination” applicable everywhere, or assuming a complete switching from traditional biomass use to modern fuels, computational modeling of neighborhood-scale pollution dispersion in a rural town in the Purepecha region of Mexico was undertaken. The objective of the study is to evaluate culturally and socioeconomically appropriate stacking options suited to different packing densities in the community.<sup>12</sup> Subsequent results from the modelled scenarios were used to develop approaches to estimate regional impacts of neighborhood pollution in ~30 surrounding towns in the Purepecha region which allow more refined regional exposure and health impact estimates. Developing tools to allow regional estimation of the neighborhood scale PM<sub>2.5</sub> pollution using readily accessible information serves as the first step in incorporating neighborhood pollution in burden of disease estimates.<sup>13</sup>

## 2 Methodology

To identify clean stacking options suited to different built environments, this study uses Quick Urban & Industrial Complex (QUIC) models to simulate pollution flow and dispersion through the built environment of a village Cucuchuco in the Purepecha region. The village consists of a gradient of different packing densities. Governing equations for QUIC-URB and QUIC-PLUME are described in Section 1 in the ESI.<sup>†</sup> The contribution of household cooking to neighborhood scale area pollution levels was estimated for a baseline scenario using traditional fuels, a business-as-usual scenario with transition of fuels to a combination of solid fuels and LPG, and 4 different “clean stacking” scenarios that reflect possible different intervention strategies for communities in the Central Highlands of rural Mexico.

### 2.1 Model evaluation – water channel experiment

To validate the QUIC simulation of turbulence fields, controlled comparisons were conducted between simulated flow structures in QUIC and directly visualized flow structures in a water channel using fluorescent dyes. To achieve similarity of water channel experiment and QUIC simulations, scaling factors are deployed to scale the water channel experiment into real world size, which is simulated by QUIC model. The QUIC modeling setup features a domain size of 50 m (X) × 50 m (Y) × 20 m (Z), with a grid resolution of 0.1 m. The QUIC domain scaling factor was 50 : 1 in relation to the physical dimensions of the building in the water channel. In the QUIC simulation, buildings are 5 meters high and spaced 10 meters apart (Fig. S1†). The wind velocity in the simulation is 5 m s<sup>-1</sup>, whereas the flow velocity in the lab is approximately 5 cm s<sup>-1</sup>. The emission source in the simulation releases 74 mg min<sup>-1</sup> pollutants from the upstream building, while in the water tank, the dye injection source has a volumetric flow rate of 360 mL min<sup>-1</sup>. All equations that govern the scaling of the water channel are presented in the ESI Section 2.<sup>†</sup> The black light and fluorescent dyes were deployed to visualize pollutant dispersion in the water channel. The reflective tracer dye intensities were captured by visible-light camera, which allowed the mapping of the pollution dispersion. Image processing techniques were then applied to determine the dye concentration. The highest reflective intensity of the dye at the emitted point is equivalent to the known maximum concentration at the same point. The concentrations in other spots were linearly scaled based on the relative reflective intensity of the tracer dye. This approach has been previously used in other studies.<sup>14,15</sup> More information about the experiment setup (schematic in Fig. S2†) and scaling methods is in Section 2 of the ESI.<sup>†</sup>

### 2.2 Study location

The town of Cucuchuco is in the Tzintzuntzan Municipality, on the shores of Patzcuaro Lake in the Purepecha region of Mexico (see Fig. S3†) at about 2040 meters above sea level, with a population of around 1200 people. Cucuchuco was selected from an evaluation of 100 communities in the area using

satellite images available through Google earth based on proximity of meteorological data, local topography and distribution of packing densities from low to high aligned with dominant wind direction.

### 2.3 Model domain

A  $600\text{ m} \times 800\text{ m}$  region was developed in QUIC city builder which was divided into a grid of  $0.5\text{ m} \times 0.5\text{ m}$  blocks. The town of Cucuchucho was constructed in the domain based on satellite imagery for building location (Fig. S4(a)†). Field teams took photographs in each street in the domain and known heights were used to extrapolate to other structures to estimate all building structures. Fig. 1 shows an estimation of building heights in the domain with the combination of field measurements, photography, and extrapolation. Emission sources were located for each building designated as a residential building, and the location of the emission source was placed where the kitchen was estimated to be (see Fig. S4(b)†). Non-residential buildings were not allocated emissions sources as the principal objectives were to model impacts of household solid fuel use. A linear vertical grid with a spacing of  $0.5\text{ m}$  was constructed with maximum height of 50 meters to reflect real distance above ground level. As with most QUIC urban simulations, logarithmically decreasing wind speed was mapped to the vertical grid with height from a reference measurement height of 10 m, since wind speed decreases logarithmically as approaching the ground.

### 2.4 Packing density

Fig. 2 shows the 3D representation of the buildings developed in city builder. The average distance between buildings has been computed and categorized to different packing density areas. The building samples were selected from the closest buildings within a region. The packing density areas are categorized as low, medium, and high for average housing distances of  $60\text{--}100$  meters,  $20\text{--}40$  meters, and less than 20 meters, respectively.

### 2.5 Model meteorology

Meteorological conditions play a major role in  $\text{PM}_{2.5}$  dispersion and deposition.<sup>9</sup> Meteorological parameters including temperature, wind speed (WS), wind direction (WD), and relative

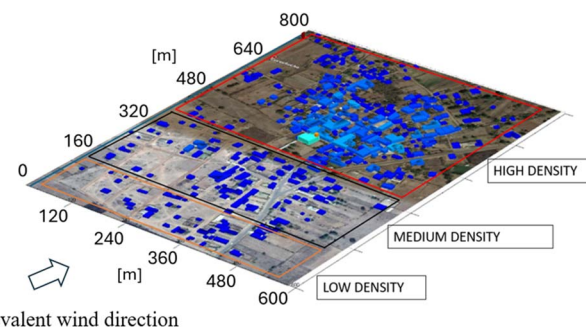


Fig. 2 Division of low, medium & high-density regions.

humidity (RH), obtained for July–August 2022 from the Morelia monitor station ( $\text{N } 19^{\circ}30'0''$ ,  $\text{W } 101^{\circ}15'0''$ ), which is located nearby the study region ( $\text{N } 19^{\circ}58'44''$ ,  $\text{W } 101^{\circ}63'43''$ ). The predominant wind direction of south-southwest ( $202.5^{\circ}$ ) is deployed in the simulation as indicated in Fig. S5.† The main cooking period coincides with periods when wind speeds are low. Simulations were conducted at  $2\text{ m s}^{-1}$  as it is the average wind speed during cooking times.

Fig. S6† presents the diurnal wind speed patterns, which shows that wind speeds are low combined with low mixing height in the early morning, and subsequently build in the afternoon, reaching a peak at around 3 pm. Based on field surveys the majority of cooking activity in this region occurs in the morning when residents cook food for breakfast lunch and dinner for an average period of  $259 \pm 123$  minutes.<sup>16</sup> Result simulations were conducted for July–August wherein the average temperature and relative humidity were  $273.15\text{ K}$  and  $0.3$  respectively.

### 2.6 Model emissions and stove types

Emission measurements were conducted in a test kitchen for different stove stacking combinations that represent the most comprehensive look at emissions from different stacking combinations in Mexico.<sup>3</sup> Emissions from houses were released from the rooftop of the house. Stove stacking combinations are shown in Table 1. The baseline scenario represents usage of traditional fuels and stoves in all packing density regions in a village. Continuation of the current trends in stove and fuel adoption forms the business-as-usual scenario where there is



Fig. 1 Building heights references.



Table 1 The emission rate from different stacking combinations

Emission rate from different stacking combination [mg min <sup>-1</sup> ]						
Stacking						
Packing density	Baseline <sup>a</sup>	BAU <sup>b</sup>	Scenario 1 <sup>c</sup>	Scenario 2 <sup>d</sup>	Scenario 3 <sup>e</sup>	Scenario 4 <sup>f</sup>
High density	TSF + LPG (324 ± 86)	LPG (0.1 ± 0.1)	LPG (0.1 ± 0.1)	P + LPG (43 ± 7)	LPG (0.1 ± 0.1)	LPG (0.1 ± 0.1)
Medium density	TSF (450 ± 63)	TSF + LPG (324 ± 86)	P + LPG (43 ± 7)	P (74 ± 43)	P + LPG (43 ± 7)	G (25 ± 3)
Low density	TSF (450 ± 63)	TSF + LPG (324 ± 86)	TSF + LPG (324 ± 86)	P (74 ± 43)	P + LPG (43 ± 7)	P + LPG (43 ± 7)

<sup>a</sup> Baseline – traditional stoves fires (TSF) in low, medium density area with some LPG in high density areas. <sup>b</sup> BAU (business as usual) – increased LPG penetration in dense urban areas, and mixed use with TSF in lower density areas. <sup>c</sup> Scenario 1 – LPG penetration in high density areas, Patsari (P) use in medium packing densities and continued use of TSF in low packing densities. <sup>d</sup> Scenario 2 – Patsari stoves in all areas – mixed use with LPG in high density areas. <sup>e</sup> Scenario 3 – LPG penetration in high density areas, Patsari with LPG dissemination in middle and low density areas. <sup>f</sup> Scenario 4 – LPG penetration in high density areas, gasifier dissemination in middle density and Patsari and LPG in low density areas.

increased Liquefied Petroleum Gas (LPG) penetration in village centers (high density areas) and continued use of traditional stoves and fuels with some LPG use for shorter tasks in outlying areas (low density areas). Scenarios 1–4 represent culturally and socioeconomically appropriate interventions in these communities with more advanced stoves progressively used from Scenario 1 to 4. Specific quantity and type of food items cooked with each stove that represent typical consumption patterns for this region are shown in Table S1,† the stove types are in Fig. S7.† Mean emission factors for each stove stacking combination are shown in Table 1 for each stove stacking combination.

Detailed presentations of emissions measurements using double hoods to separately estimate direct and fugitive emissions in a simulated kitchen have been provided elsewhere.<sup>3</sup> Briefly, PM<sub>2.5</sub> emission factors were measured gravimetrically for each stove stacking combination using a 102 mm fiberglass filter at a sample flow rate of 16.7 L min<sup>-1</sup> for chimney emissions.<sup>16</sup> The simulated kitchen was representative of local kitchens in terms of building material, size, volume, and air exchange rates.

## 2.7 Neighborhood scale area concentrations and perimeter concentrations

The results of the simulations for two metrics are presented: (a) area average concentration describes the average PM<sub>2.5</sub> concentration for each packing density area in the domain, including areas that are agricultural. The QUIC simulation allows simulation of packing zones independently with sources from other zones switched off, and thus the contributions from upstream packing densities can be isolated from local emissions. In this way, quantification, and assessment of neighborhood emission contributions from different packing densities is possible, which is not possible from direct environmental monitoring using smart sensors or similar approaches; and (b) average perimeter concentration reflect the average concentration around the perimeter of the house 0.5 m away from walls at the height of 1 m. Average perimeter concentrations reflect concentrations of PM<sub>2.5</sub> that are available for infiltration into a home during cooking events, which are relevant for models to estimate impacts on indoor air concentrations and subsequently exposures.

## 2.8 Statistical model

A statistical model was developed that can be applied to different communities across a region based on the simulation conducted for Cucuchucho (refer to the result section for more details). Since communities across the region do not have the same packing densities, built structures, or populations, changes in the proportions of different density areas are incorporated into this model. The equations are functions of house density and spatial average pollution concentrations. Both local and neighborhood pollution estimation is specific to the areas and packing densities of each individual community. Pollution concentrations for different building densities in different communities can be estimated by the following equation:

$$\left\{ \begin{array}{l} C_{\text{local}} = 0.15 \times \rho_{\text{local}} - 35.273 \\ C_{\text{from neighbor}} = \frac{(0.0165 \times \rho_{\text{neighbor}} - 4.6)}{A_{\text{local}}} \end{array} \right.$$

where  $\rho_{\text{local}}$  is the local building density, defined by the number of households divided by the area ( $A_{\text{local}}$ ).  $\rho_{\text{neighbor}}$  is the building density in the immediate upwind neighborhood.  $C_{\text{local}}$  indicates the spatial average concentration from local emitted pollutants, which is linearly correlated to the local household packing density.  $C_{\text{from neighbor}}$  represents the pollution contribution from the upstream neighborhood community, which is linearly correlated to the neighbor community household packing density normalized by local area. One model depicts local concentration, while the other represents neighborhood influence and as such is normalized by the relevant local area. Both local and neighborhood pollution estimation is specific to each individual community based on building densities. The statistical model is not dependent on a specific wind direction, as it allows for independent selection of local and neighborhood packing densities.

## 3 Results and discussion

### 3.1 Comparison of laboratory and numerical modeling

Fig. 3(a) and (b) present the comparison of pollution dispersion in a building wake from water channel experiments and from

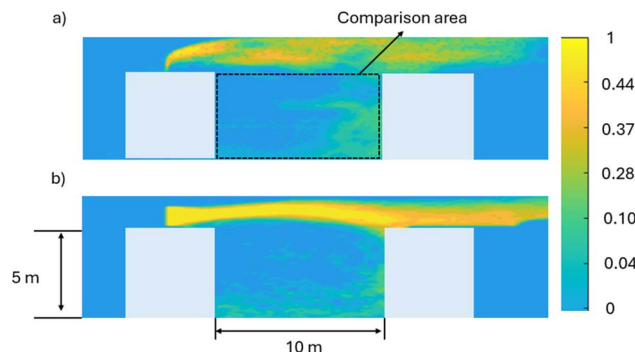


Fig. 3 Concentration distribution of pollutants in the building wake (a) water channel experiment (b) QUIC modeling.

QUIC modeling, respectively. The background concentration from the water tank experiment is denoised and concentration values are scaled as a fraction of the maximum value, the scale bar represents the concentration as a percentage. Concentration profiles between QUIC simulation and the water channel are similar in trapping pollutants between the buildings. As indicated in the figure, the pollutants accumulate with the backflow downwind of the upstream building, indicating that this recirculation in the building wakes traps stove emissions for a longer duration. This street canyon serves as the basic geometric unit in urban or suburban regions. The configurations of a village are approximately repetitions of such street canyon units. The presence of buildings leads to larger vertical mixing of the pollutants compared to flat terrain, thus contributing to the near-ground pollution concentration. This pooling effect in different wake distance is presented in Fig. S8 and the flow effects are described in ESI Section 6.† The QUIC model is designed to simulate pollutant dispersion patterns in urban and industrial environments, with a primary focus on how pollutants spread and interact with surrounding structures and atmospheric conditions. The model's strength lies in providing a realistic depiction of the dispersion behavior rather than precisely modeling the source characteristics. Therefore, while discrepancies may appear near the source due to simplifications and assumptions made for computational needs and efficiency, the critical output shows good agreement between the simulation and water channel in the comparison area.

Fig. 4 demonstrates the statistical point-by-point comparison between the water channel and QUIC numerical modeling results in the building wake comparison area. Overall, QUIC-PLUME model provides a reasonable estimate of dispersion trends in the building wake.

In addition to this comparison, the QUIC model has been validated previously through various methods, including comparisons with field measurements and controlled experiments. For example, QUIC flow patterns were compared to those observed in a wind tunnel experiment involving complex arrays of buildings. The model successfully simulated key flow characteristics, including channeling and recirculation patterns within specific street canyons.<sup>17</sup> The results demonstrated the model's capability to simulate complex urban flows.

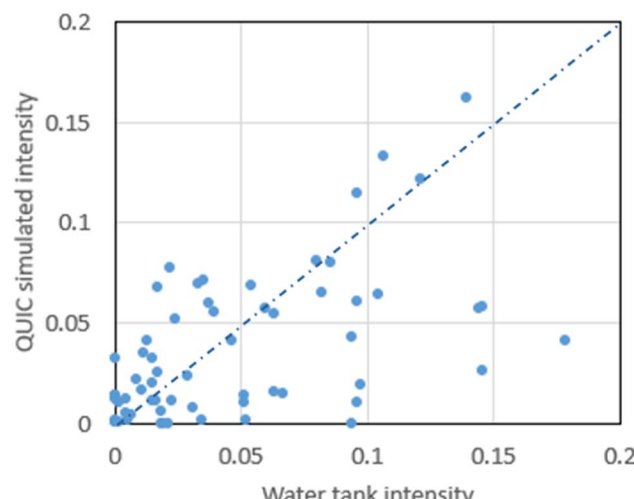


Fig. 4 Point-by-point comparison of QUIC modeled and water tank simulated concentration.

QUIC-PLUME modeled pollution distribution results were compared with the Joint Urban 2003 field experiments in downtown Oklahoma City using a point source release for eight intensive operating periods of 30 minutes duration. A threshold dosage method was used to examine the percentage of samplers that QUIC-PLUME correctly predicted to be above the threshold, which obtained 83% matches in the 24 tracer experiments.<sup>18</sup>

### 3.2 Stacking scenario results during cooking events

The scenarios evaluated with the current simulations compare 4 progressive development scenarios using clean stacking combinations compared to business as usual expected to occur in the next decade. The simulated scenarios reflect a range of feasible “clean stacking” options for interventions that can be distributed into the different areas of the community to examine the impacts on neighborhood contributed concentrations in each area. Fig. 5 shows QUIC simulation of  $\text{PM}_{2.5}$  concentrations in Cucuchucho under scenarios corresponding to Table 1. The average area concentration over the whole domain are: (a)  $83.15 \mu\text{g m}^{-3}$ ; (b)  $34.86 \mu\text{g m}^{-3}$ ; (c)  $14.75 \mu\text{g m}^{-3}$ ; (d)  $14.73 \mu\text{g m}^{-3}$ ; (e)  $4.66 \mu\text{g m}^{-3}$ ; (f)  $3.49 \mu\text{g m}^{-3}$ .

Fig. 5 also shows the dependency of  $\text{PM}_{2.5}$  concentrations on the predominant wind direction and the number of emission sources at a height of 1 m above ground. Windward sides of the buildings are affected by the upstream emissions and the leeward side tends to trap emissions from each individual household. In general, the scenario analysis evaluates the impacts of programs that include interventions in the lower packing densities, in relation to Scenario 1, which shows a program focused on LPG penetration in high density areas with use of traditional stoves in lower packing densities. The benefits of LPG use in high density areas are largely mitigated by upstream use of traditional stoves. Scenario 2 shows the use of Patsari chimney stoves in all packing densities, the upstream pollution contribution is non negligible in high packing density. Scenarios 3 and 4 show the dissemination of LPG in



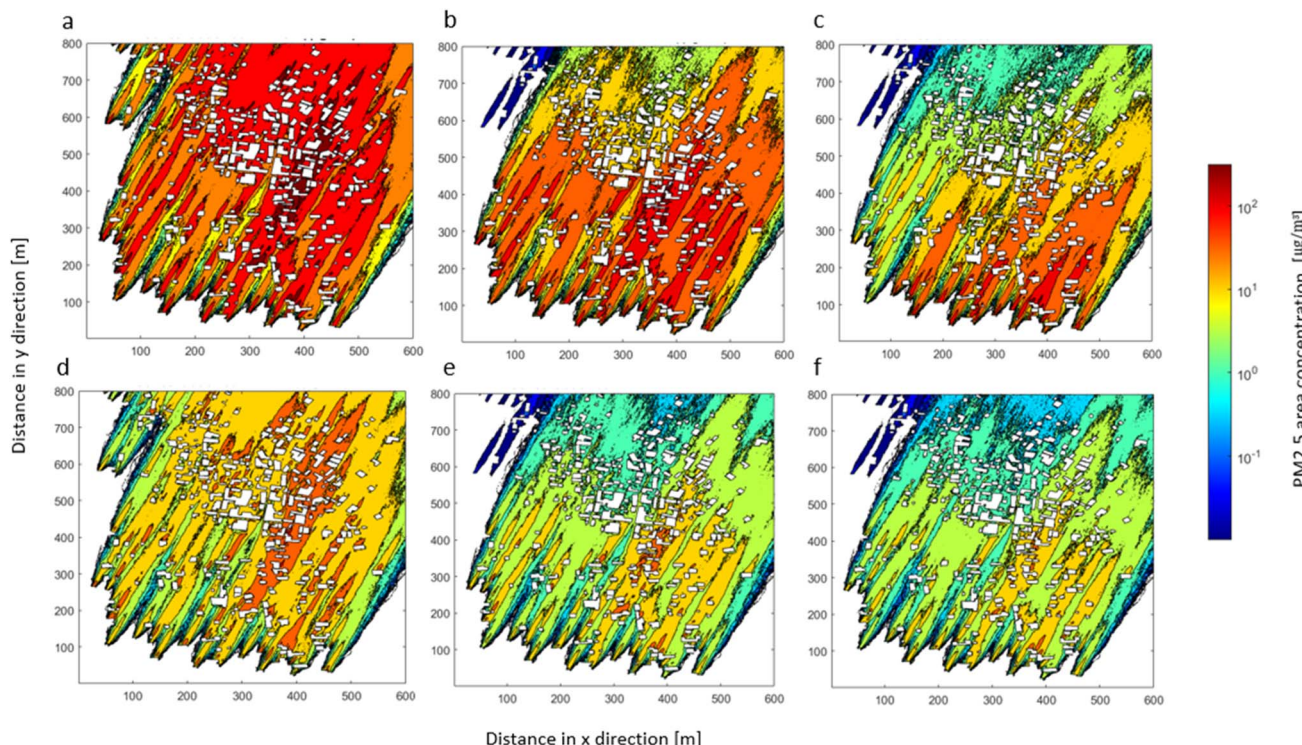


Fig. 5 Pollution dispersion at 1 m height in different stacking scenarios during cooking events with prevalent wind direction of SSW. (a) Baseline; (b) BAU; (c) Scenario 1; (d) Scenario 2; (e) Scenario 3; (f) Scenario 4.

high density areas combined with dissemination of chimney stoves or gasifier stoves in areas with lower packing densities. The combination of these stacking intervention approaches results in the lowest air pollution concentrations. Scenario 4 resulted in the most effective control of PM<sub>2.5</sub> concentrations in all three density regions. Compared with the BAU scenario, the implementation of Scenario 4 reduced area concentrations by approximately 89% and achieved WHO guideline concentrations in urban areas from local emissions. Clean burning semi gasifier chimney stoves should be explored further as they lead to significant reductions in neighborhood pollution impacts. In addition, adoption dynamics and mechanisms to increase sustained use of cleaner alternatives (carbon offset programs, social benefits *etc.*) play a significant role in determining the degree to which benefits are realized.

### 3.3 Neighborhood source contributions

Fig. 6 shows the relative percentage of neighborhood concentrations contributed by each packing density for baseline scenario, which reflects the current situation in Cucuchucho. Approximately one third of PM<sub>2.5</sub> concentrations are attributed to houses upstream in medium and high-density areas of the village. In the medium packing density area, the emissions from dispersed upstream homes (low-packing density area) contribute 28% to PM<sub>2.5</sub> pollution, defined as imported neighborhood pollution. In the high packing density area, both low and medium packing density areas are located upwind and imported neighborhood pollution contributes 20% and 4% of PM<sub>2.5</sub> pollution concentrations respectively.

Fig. 7 presents area averaged local emissions and contributions from upstream packing densities under each scenario. Since simulations do not include sources upstream of the low-density area, in each of the scenarios, upstream emissions are zero for low density areas. In the Baseline scenario, the PM<sub>2.5</sub> area average concentration in the high-density area is 103  $\mu\text{g m}^{-3}$  with 33% contributed from the upstream community. In the business-as-usual (BAU) scenario, with the increased penetration of LPG in the high-density area and mixed open fire in other areas the overall ambient PM<sub>2.5</sub> concentration decreased down to  $\sim 25 \mu\text{g m}^{-3}$  with 99% contributed from the upstream neighborhood. Even without regional background

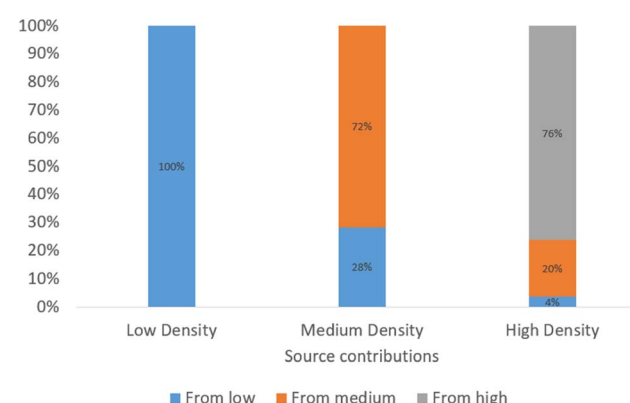


Fig. 6 The percentage of neighborhood pollution concentration contributed by upstream packing densities for baseline scenario.



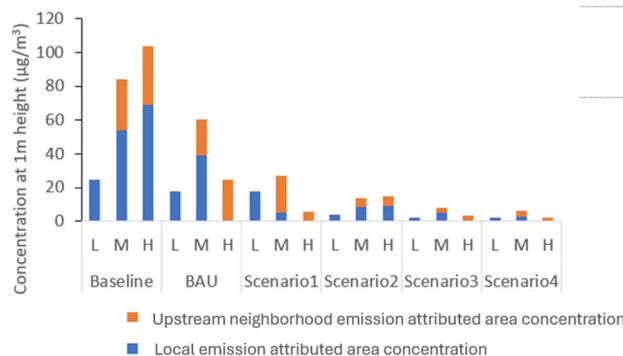


Fig. 7 Spatial averaged pollution concentrations contributed by upstream communities under scenarios defined in Table 1 (L: low-packing density area; M: medium-packing density area; H: high-packing density area).

contributions, the neighborhood pollution transported into these high-density areas is approximately equivalent to the WHO interim target 2 of  $25 \mu\text{g m}^{-3}$ . Under the implementation of Scenario 3 or 4, with sufficient control in all three density areas, the air quality guideline of less than  $5 \mu\text{g m}^{-3}$  from local sources could be achieved in high-density urban areas with concentrations of  $2.39 \mu\text{g m}^{-3}$  and  $\sim 3 \mu\text{g m}^{-3}$  respectively. Concentrations in medium density packing areas were  $8.07$  and  $6.12 \mu\text{g m}^{-3}$  respectively. Achieving these concentrations in practice, however, is dependent on the degree to which the stove stacking interventions are adopted and used (Table 1), meteorology, and the presence of other emissions sources in the area that are not quantified in this simulation.

To estimate indoor impacts through infiltration, the perimeter concentrations around each home averaged for each packing density are presented in Fig. S9.† Table S2† presents the data table with area concentrations and perimeter concentrations for each scenario. A more practical adoption rate scheme is presented in Table S3,† and the corresponding perimeter concentrations is in Fig. S10.†

### 3.4 Regional estimates of neighborhood pollution impacts

To apply these results to other settlements within the Purepecha region, a statistical model to estimate regional neighborhood pollution impacts was developed as a first step in incorporation of neighborhood pollution in estimates of regional health burdens from household pollution (see Section 2.8). The density factor defined below based on readily available information was applied to normalize both direct local emission contributions and contributions from upstream neighborhood.

$$\rho = \frac{\text{number of households}}{\text{community area (km}^2\text{)}}$$

Fig. 8 shows the application of this density factor ( $\rho$ ) to simulations of area pollution concentration for each packing density (low, medium and high) in Cucuchucho with distance downstream. As presented in the figure, when the area concentration is normalized by density factor, the resulting profiles of normalized concentration *versus* downstream distance exhibit similar trends across different packing densities. This suggests that area concentrations can be estimated using the density factor through linear regression. A regional estimation can be determined by summing the local emissions within the community and the contributions from upstream neighborhood areas during cooking hours. The convergence of the normalized local and neighborhood concentrations along the same linear trend for different packing densities demonstrates that the statistical model outlined in Section 2.8 of the methodology can be applied to other communities within the region.

### 3.5 Application to other communities

The statistical model to estimate both local emission concentrations and neighborhood concentrations in relation to packing density factor is shown in Fig. 9. The model is described in methodology Section 2.8. Based on regression

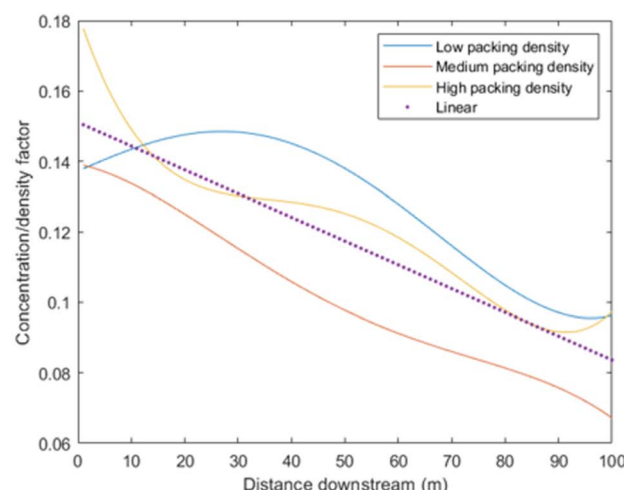
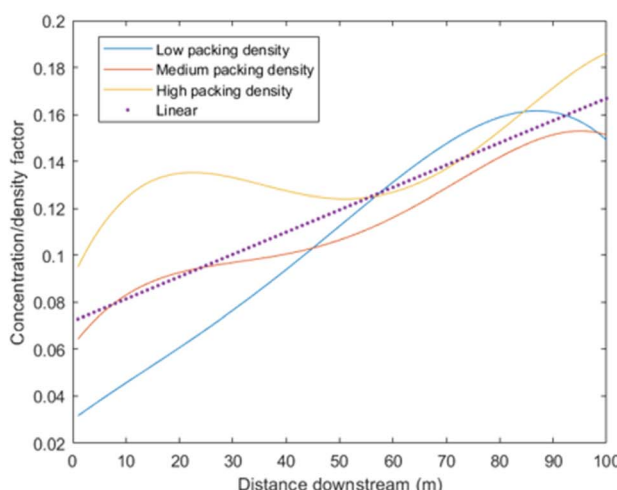


Fig. 8 Normalized PM<sub>2.5</sub> concentration with distance downstream (a) only consider local emission sources (b) only consider upwind neighborhood emission sources.



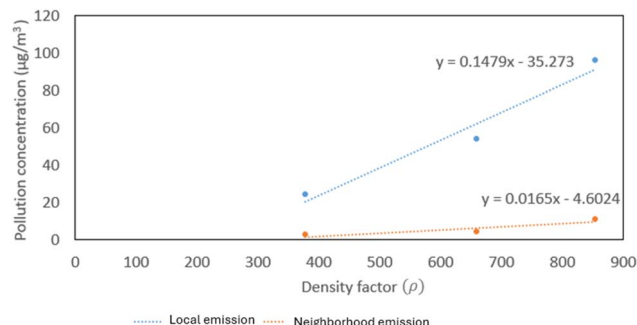


Fig. 9 Linear regression for average concentration vs. density factor.

intercepts, the distance between homes where neighborhood contributions from use of traditional stoves do not substantially impact downwind community is 70 m. Thus, for communities where homes are apart further than 70 m, the pollutants effects would not be expected to impact near neighborhood ambient air quality. Clearly, however this is dependent both on the emission rate for the specific stove technology and average wind speed. While wind speed had a strong impact on the concentration, as Fig. S11† shows, the proportional reduction in pollution concentration is similar for different density factors (high, medium and low) upon different wind speeds. This allows for wind speed adjustment to be incorporated into the model for different communities as follows:

$$R_w = (-0.217) \times U + 1.434$$

$$C_{\text{total}} = R_w \times (C_{\text{base}})$$

where  $R_w$  is the adjusting ratio of wind speed,  $U$  is the corresponding wind speed in the specific village,  $C_{\text{base}}$  is the baseline concentration at  $2 \text{ m s}^{-1}$  derived from our statistical model.

Since the density factor is readily obtainable from regional data for Purepecha communities, impacts of neighborhood pollution concentrations at a regional scale can be estimated for incorporation into burden of disease assessments. To demonstrate this approach, estimation of impacts of neighborhood pollution concentrations for a sample of 29 communities surrounding Cucuchucho was performed using mapped areas of each community using satellite imagery on Google maps. In this case study of the Purepecha region, we assume wind travels from lower densities on the outskirts to higher densities in village centers. Across these communities, the population range from 453 to 13 610, and areas range from  $0.14$  to  $2.2 \text{ km}^2$ . While in reality, there are clearly individual communities with different built environment from this idealized structure, which results in localized areas in the community having an average concentration higher or lower than expected from model estimates. When applied regionally, however, these uncertainties would not be expected to result in systematic bias, which allows for deployment of current models in burden of disease estimates.

Fig. 10 shows estimated contributions of (a) direct emissions and (b) neighborhood pollution to overall  $\text{PM}_{2.5}$  ambient concentrations for the surrounding communities in the Purepecha region using traditional stoves. The model estimates demonstrate that neighborhood pollution contributes significantly to ambient  $\text{PM}_{2.5}$  concentrations in these communities, but the geographical scale of this impact is rarely accounted for in burden of disease assessments. Fig. 10(b) highlights the village of Comachuén which was estimated to have contribution from the upstream neighborhood of  $\sim 30\%$  when using traditional stoves for cooking. Field measurements of 24 hour average  $\text{PM}_{2.5}$  ambient pollution concentrations in the center of Comachuén were  $59 \mu\text{g m}^{-3}$  during the period November 2004–January 2005 when the community used traditional stoves.<sup>19</sup> During this period the average wind speed was  $3 \text{ m s}^{-1}$

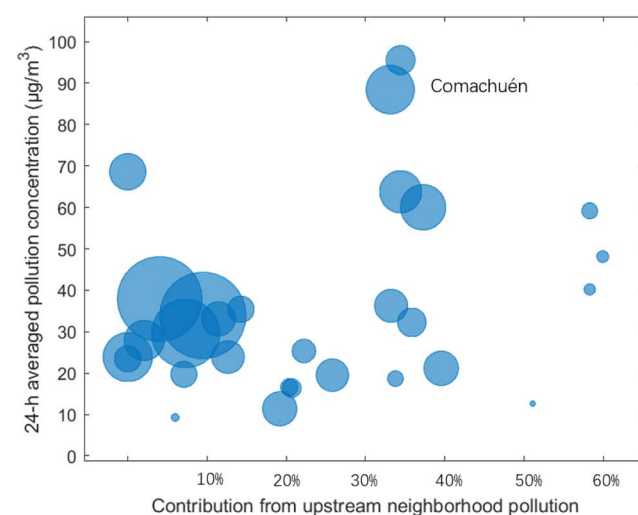
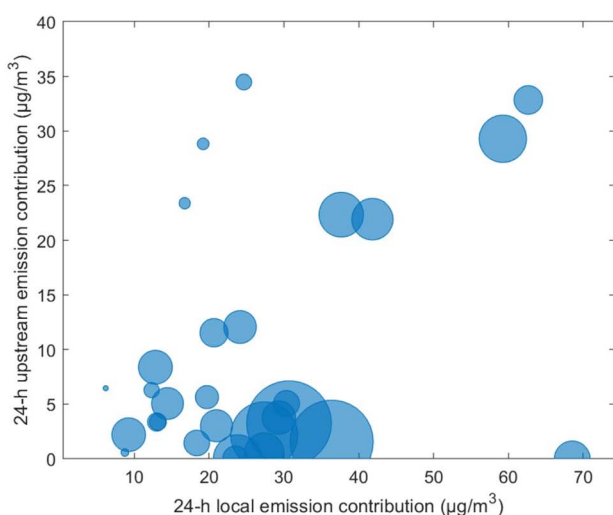


Fig. 10 Baseline scenario (a). Comparison of the local emitted  $\text{PM}_{2.5}$  concentration and the upstream neighborhood emitted concentration (b). Contribution from neighborhood pollution in different communities. Note: bubbles are scaled to represent number of homes in each community.



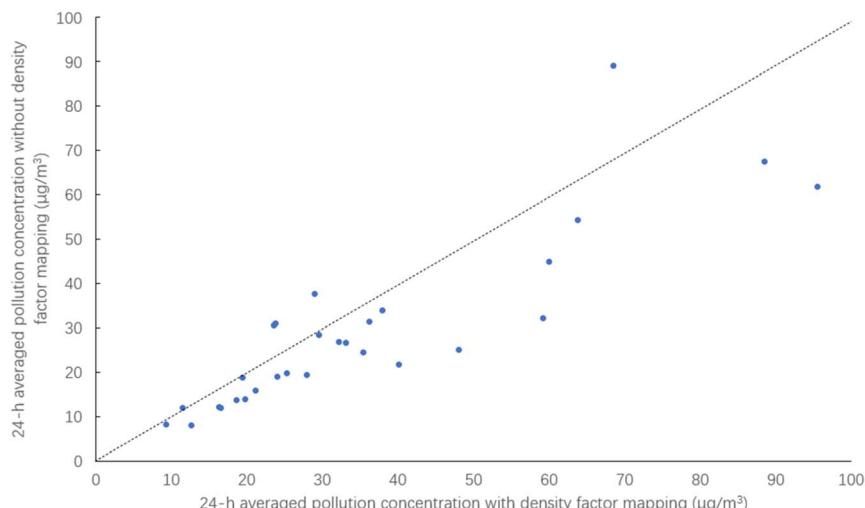


Fig. 11 Comparison of 24 h mean concentrations estimated using with and without mapping of packing densities.

(Fig. S12,†). When adjusted for wind speed the area concentration estimated from the statistical model was estimated to be  $\sim 60 \mu\text{g m}^{-3}$ , showing good agreement between measured and modelled concentrations.

Since mapping the packing densities on satellite imagery in Google maps is time intensive for application on a regional basis, estimates of ambient  $\text{PM}_{2.5}$  concentrations these communities were compared to approaches that just apply a density factor from available data with no community mapping of packing densities. Fig. 11 Shows a comparison of 24 h mean concentrations estimated using with and without mapping of packing densities. The figure shows that while there are individual communities that are over and underestimated using this approach, the estimates on a regional wide basis agree well using both approaches which will allow broader application to estimate disease burdens on a regional basis.

## 4 Conclusion

Overall, the results of these simulations demonstrate that neighborhood scale  $\text{PM}_{2.5}$  pollution can contribute significantly to  $\text{PM}_{2.5}$  concentrations in rural communities in the Purepecha region of Mexico and can play a significant role in mitigating the potential benefits of interventions designed to reduce health impacts from  $\text{PM}_{2.5}$  exposures in more urbanized communities. Intervention programs should also target upstream homes in more dispersed packing densities with socioeconomic and culturally appropriate interventions to maximize benefits of LPG in more urbanized centers of communities. The results also show that impacts of neighborhood scale  $\text{PM}_{2.5}$  pollution from solid fuel use on health are significant and approaches are needed to include health impacts in regional and global burden of disease estimates. Like modelling frameworks that allow health impacts from household air pollution to be included in burden of disease estimates, the current analysis demonstrates that statistical modeling frameworks can be applied at a regional level to

estimate impacts of neighborhood  $\text{PM}_{2.5}$  pollution on regional health burdens based on current stove stacking patterns. Since stove stacking has been demonstrated globally, these frameworks allow for systematic evaluation of the interaction between packing density, neighborhood scale pollution concentrations and impacts on disease burdens.<sup>20</sup>

## Data availability

Model analysis for predicting  $\text{PM}_{2.5}$  concentrations from solid fuel burning in rural areas. The study integrates local emissions and neighborhood impacts to improve air quality assessments. Data for this article, the emission inventories are available at <https://doi.org/10.1021/acs.est.8b01704>. The data supporting this article has been included as part of the ESI.† The software Quick Urban & Industry Complex can be found at <https://www.lanl.gov/projects/quic/>. We are grateful to the Los Alamos National Laboratory for providing the QUIC model under license number: LIC-20-04147.

## Conflicts of interest

There are no conflicts to declare.

## References

- 1 O. R. Masera, R. Díaz and V. Berrueta, From cookstoves to cooking systems: the integrated program on sustainable household energy use in Mexico, *Energy Sustainable Dev.*, 2005, **9**(1), 25–36, DOI: [10.1016/S0973-0826\(08\)60480-9](https://doi.org/10.1016/S0973-0826(08)60480-9).
- 2 A. Schilmann, *et al.*, A follow-up study after an improved cookstove intervention in rural Mexico: Estimation of household energy use and chronic  $\text{PM}_{2.5}$  exposure, *Environ. Int.*, 2019, **131**, 105013, DOI: [10.1016/j.envint.2019.105013](https://doi.org/10.1016/j.envint.2019.105013).
- 3 V. M. Berrueta, M. Serrano-Medrano, C. García-Bustamante, M. Astier and O. R. Masera, Promoting sustainable local development of rural communities and mitigating climate



change: the case of Mexico's Patsari improved cookstove project, *Clim. Change*, 2017, **140**(1), 63–77, DOI: [10.1007/s10584-015-1523-y](https://doi.org/10.1007/s10584-015-1523-y).

4 N. Kalu, N. Lufesi, D. Havens and K. Mortimer, Implementation of World Health Organization Integrated Management of Childhood Illnesses (IMCI) Guidelines for the Assessment of Pneumonia in the Under 5s in Rural Malawi, *PLoS One*, 2016, **11**(5), e0155830, DOI: [10.1371/journal.pone.0155830](https://doi.org/10.1371/journal.pone.0155830).

5 A. Van Donkelaar, *et al.*, Global Estimates of Fine Particulate Matter using a Combined Geophysical-Statistical Method with Information from Satellites, Models, and Monitors, *Environ. Sci. Technol.*, 2016, **50**(7), 3762–3772, DOI: [10.1021/acs.est.5b05833](https://doi.org/10.1021/acs.est.5b05833).

6 A. Pandey, *et al.*, Health and economic impact of air pollution in the states of India: the Global Burden of Disease Study 2019, *Lancet Planet. Health*, 2021, **5**(1), e25–e38, DOI: [10.1016/S2542-5196\(20\)30298-9](https://doi.org/10.1016/S2542-5196(20)30298-9).

7 A. Van Donkelaar, *et al.*, Monthly Global Estimates of Fine Particulate Matter and Their Uncertainty, *Environ. Sci. Technol.*, 2021, **55**(22), 15287–15300, DOI: [10.1021/acs.est.1c05309](https://doi.org/10.1021/acs.est.1c05309).

8 I. Stasiulaitiene, *et al.*, Infiltration of outdoor combustion-generated pollutants to indoors due to various ventilation regimes: A case of a single-family energy efficient building, *Build. Environ.*, 2019, **157**, 235–241, DOI: [10.1016/j.buildenv.2019.04.053](https://doi.org/10.1016/j.buildenv.2019.04.053).

9 H. Zhang, Y. Wang, J. Hu, Q. Ying and X. M. Hu, Relationships between meteorological parameters and criteria air pollutants in three megacities in China, *Environ. Res.*, 2015, **140**, 242–254, DOI: [10.1016/j.envres.2015.04.004](https://doi.org/10.1016/j.envres.2015.04.004).

10 I. Ruiz-Mercado and O. Masera, Patterns of Stove Use in the Context of Fuel–Device Stacking: Rationale and Implications, *EcoHealth*, 2015, **12**(1), 42–56, DOI: [10.1007/s10393-015-1009-4](https://doi.org/10.1007/s10393-015-1009-4).

11 K. An, S.-M. Wong and J. C.-H. Fung, Exploration of sustainable building morphologies for effective passive pollutant dispersion within compact urban environments, *Build. Environ.*, 2019, **148**, 508–523, DOI: [10.1016/j.buildenv.2018.11.030](https://doi.org/10.1016/j.buildenv.2018.11.030).

12 R. Edwards, M. Princevac, R. Weltman, M. Ghasemian, N. K. Arora and T. Bond, Modeling emission rates and exposures from outdoor cooking, *Atmos. Environ.*, 2017, **164**, 50–60, DOI: [10.1016/j.atmosenv.2017.05.029](https://doi.org/10.1016/j.atmosenv.2017.05.029).

13 Y. He, S. R. Nishandar, R. D. Edwards and M. Princevac, Air Quality Modeling of Cooking Stove Emissions and Exposure Assessment in Rural Areas, *Sustainability*, 2023, **15**(7), 5676, DOI: [10.3390/su15075676](https://doi.org/10.3390/su15075676).

14 B. Di Bella, M. Khatamifar and W. Lin, Experimental study of flow visualisation using fluorescent dye, *Flow Meas. Instrum.*, 2022, **87**, 102231, DOI: [10.1016/j.flowmeasinst.2022.102231](https://doi.org/10.1016/j.flowmeasinst.2022.102231).

15 H. Pan, X. Li and M. Princevac, *PIV and PLIF Measurements of Model Urban Flows in a Water Channel*, 2007, DOI: [10.1115/FEDSM2007-37671](https://doi.org/10.1115/FEDSM2007-37671).

16 V. M. Ruiz-García, *et al.*, Fugitive Emissions and Health Implications of Plancha-Type Stoves, *Environ. Sci. Technol.*, 2018, **52**(18), 10848–10855, DOI: [10.1021/acs.est.8b01704](https://doi.org/10.1021/acs.est.8b01704).

17 M. J. Brown, *Quick Urban and Industrial Complex (QUIC) CBR Plume Modeling System: Validation-Study Document*, LA-UR-18-29993, 2018, p. 1479898, DOI: [10.2172/1479898](https://doi.org/10.2172/1479898).

18 M. Princevac, *et al.*, Field, laboratory and numerical study of transportation emissions in built environments surrounding major arterials in Southern Californian Cities, in *Proceeding of Sixth International Symposium on Turbulence and Shear Flow Phenomena*, Seoul National University, Begellhouse, Seoul, Korea, 2009, pp. 459–464, DOI: [10.1615/TSFP6.720](https://doi.org/10.1615/TSFP6.720).

19 M. Zuk, *et al.*, The impact of improved wood-burning stoves on fine particulate matter concentrations in rural Mexican homes, *J. Expo. Sci. Environ. Epidemiol.*, 2007, **17**(3), 224–232, DOI: [10.1038/sj.jes.7500499](https://doi.org/10.1038/sj.jes.7500499).

20 A. V. Shankar, *et al.*, Everybody stacks: Lessons from household energy case studies to inform design principles for clean energy transitions, *Energy Policy*, 2020, **141**, 111468, DOI: [10.1016/j.enpol.2020.111468](https://doi.org/10.1016/j.enpol.2020.111468).

